MOLECULAR AND CELLULAR BIOLOGY, Dec. 1992, p. 5690–5699
0270-7306/92/125690-10$02.00/0

Vol. 12, No. 12

Yeast *RHO3* and *RHO4 ras* Superfamily Genes Are Necessary for Bud Growth, and Their Defect Is Suppressed by a High Dose of Bud Formation Genes *CDC42* and *BEM1*

YASUSHI MATSUI* AND AKIO TOH-E

Department of Biology, University of Tokyo, 7-3-1, Hongo, Bunkyo-ku, Tokyo 113, Japan

Received 23 June 1992/Returned for modification 6 August 1992/Accepted 20 September 1992

***RHO3* and *RHO4* are members of the *ras* superfamily genes of the yeast *Saccharomyces cerevisiae* and are related functionally to each other. Experiments using a conditionally expressed allele of *RHO4* revealed that depletion of both the *RHO3* and *RHO4* gene products resulted in lysis of cells with a small bud, which could be prevented by the presence of osmotic stabilizing agents in the medium. *rho3 rho4* cells incubated in medium containing an osmotic stabilizing agent were rounded and enlarged and displayed delocalized deposition of chitin and delocalization of actin patches, indicating that these cells lost cell polarity. Nine genes whose overexpression could suppress the defect of the *RHO3* function were isolated (*SRO* genes). Two of them were identical with *CDC42* and *BEM1*, bud site assembly genes involved in the process of bud emergence. A high dose of *CDC42* complemented the *rho3* defect, whereas overexpression of *RHO3* had an inhibitory effect on the growth of mutants defective in the *CDC24-CDC42* pathway. These results, along with comparison of cell morphology between *rho3 rho4* cells and *cdc24* (or *cdc42*) mutant cells kept under the restrictive conditions, strongly suggest that the functions of *RHO3* and *RHO4* are required after initiation of bud formation to maintain cell polarity during maturation of daughter cells.**

A definite cell polarity is required for many cellular processes, such as polarized secretion in nerve cells and asymmetric cell division or growth in many organisms. However, the mechanisms that determine and maintain cell polarity are not fully understood. Recently, molecular dissection of the processes involved in the determination of cell polarity has been begun, using the budding yeast *Saccharomyces cerevisiae*.

In *S. cerevisiae*, a daughter cell is produced as a bud, and bud formation is a cell cycle-regulated event that involves the establishment and maintenance of cell polarity (13, 16, 28, 29). The cytoskeleton, consisting of actin filaments and microtubules, is organized with respect to cell polarity, and cells grow asymmetrically by the subsequent polarized secretion and localized deposition of new cell wall material, resulting in the formation of buds (2, 7, 14, 42). Development of cell polarity is controlled by a network consisting of many different proteins. Several genes, such as *CDC24*, *CDC42*, and *BEM*, are known to be involved in polarity establishment and bud emergence (1, 5, 38, 39). At restrictive temperatures, the cells carrying temperature-sensitive alleles of these genes fail to form buds, grow isotropically, and continue the nuclear cycle, resulting in rounded, greatly enlarged, unbudded cells that often become multinucleated. Chitin is deposited uniformly throughout the cell wall, and the cytoplasmic actin network appears disorganized.

Molecular analysis of the genes mentioned above has been reported. *CDC42* is a member of *rho* family genes (20), which belong to the *ras* superfamily genes (3). Genetic analysis of *CDC24* (4) and biological analysis of the human homologs *dbl* and *CDC42Hs* (15, 26, 36) suggest that *CDC24* is a candidate for the gene encoding an exchange factor that regulates the GDP-GTP exchange reaction of the *CDC42* gene product. The *BEM1* gene product possesses two copies of the SH3 domain that is found in many proteins associated with the cortical cytoskeleton (11).

We recently isolated two novel *rho* family genes, *RHO3* and *RHO4* (24). While disruption of *RHO4* does not affect cell growth, cells lacking *RHO3* grow very poorly. The simultaneous disruption of both *RHO3* and *RHO4* results in inviability of cells at 30°C or above, and overexpression of *RHO4* suppresses the growth defect in *rho3* disruptants, indicating that the functions of *RHO3* and *RHO4* are related to each other.

In this report, we present evidence that the functions of *RHO3* and *RHO4* are involved in the maintenance of cell polarity after the initiation of bud formation and that these functions are required for formation of a mature daughter cell.

MATERIALS AND METHODS

Microbial techniques. Yeast transformations were performed by the method of Ito et al. (19), and other standard yeast genetic manipulations were performed as described by Sherman et al. (35). LB and 2×YT (23) were used for bacterial culture. Rich medium containing glucose (YPD) and synthetic complete medium (SC) were prepared as described by Sherman et al. (35). Other media were YPGal (YPD with 2% galactose and 0.2% sucrose instead of 2% glucose), SCGal (SC with 2% galactose and 0.2% sucrose instead of 2% glucose), SC-U (SC lacking uracil), SCGal-U (SCGal lacking uracil), and YPD+Sorb and YPGal+Sorb (YPD and YPGal, respectively, containing 1 M sorbitol). Synthetic glucose medium (SD) without a nitrogen source contained 0.6% yeast nitrogen base without ammonium sulfate (Difco) and 2% glucose. Synthetic galactose medium (SGal) without a nitrogen source contained 0.6% yeast nitrogen base without ammonium sulfate, 2% galactose, and 0.2% sucrose. When α-factor was added to a medium, the pH of the medium was adjusted at pH 4.0 and 0.1 mg of

* Corresponding author.

TABLE 1. Yeast strains used

Strain	Genotype	Reference or source
Y147	*MAT***a** *cdc24-4 ura3 leu2-3,112 his3*	4
DJTD2-16A	*MAT***a** *cdc42-1 ura3 leu2 trp1 his4*	20
YPH499	*MAT***a** *ura3-52 leu2 his3 trp1 lys2 ade2*	37
YPH500	*MAT*α *ura3-52 leu2 his3 trp1 lys2 ade2*	37
YPH501	*MAT***a**/*MAT*α *ura3-52/ura3-52 leu2/leu2 his3/his3 trp1/trp1 lys2/lys2 ade2/ade2*	37
YMR501	*MAT*α *rho3::LEU2 pGAL7:RHO4 leu2 his3 trp1 lys2 ade2*	This study
YMR502	*MAT***a** *rho3::LEU2 pGAL7:RHO4 leu2 his3 trp1 lys2 ade2*	This study
YMR505	*MAT*α *rho3::LEU2 pGAL7:RHO4 ura3::HIS3 leu2 his3 trp1 lys2 ade2*	This study
YMR509	*MAT*α *rho3::LEU2 rho4::HIS3 pGAL7:RHO4 leu2 his3 trp1 lys2 ade2*	This study
YMR510	*MAT***a** *rho3::LEU2 rho4::HIS3 pGAL7:RHO4 leu2 his3 trp1 lys2 ade2*	This study
YMR512	*MAT***a** *rho3::LEU2 pGAL7:RHO4 ura3::TRP1 leu2 his3 trp1 lys2 ade2*	This study
YMR522	*MAT***a**/*MAT*α *rho3::LEU2/rho3::LEU2 rho4::HIS3/rho4::HIS3 pGAL7:RHO4/pGAL7:RHO4 ura3::TRP1/URA3 leu2/leu2 his3/his3 trp1/trp1 lys2/lys2 ade2/ade2*	YMR509 × YMR512
YMR420	*MAT***a** *cdc42-1 ura3 leu2 his3 trp1*	Segregant of DJTD2-16A × YPH500

α-factor was added to 10 ml of culture every 2 h. Yeast cells were cultured at 30°C unless otherwise indicated.

DNA manipulation. Plasmid DNA was prepared from *Escherichia coli* DH5 according to the alkaline lysis method described by Maniatis et al. (23). Yeast DNA was prepared as described by Sherman et al. (35). Restriction enzymes were purchased from Toyobo and were used according to the manufacturer's directions. Probes for hybridization and washings of membranes were prepared as described by Maniatis et al. (23). Deletion derivatives of plasmids for sequencing were constructed by the method of Henikoff (17), and the nucleotide sequences were determined by the method of Sanger et al. (33), using the universal sequencing primer or synthetic oligonucleotides to prime the reaction.

Strains and plasmids. The principal yeast strains used are listed in Table 1 pBluescript was purchased from Stratagene. The YEp24 library (8) contains approximately 10-kb yeast genomic *Sau*3A DNA fragments inserted into the *Bam*HI site of YEp24 (6), a high-copy-number plasmid containing the *URA3* selectable marker and the 2μm plasmid origin of replication. Plasmids pSRO1 and pSRO2 are isolates from this library; they contain an approximately 8-kb fragment bearing *SRO1* and an approximately 13-kb fragment bearing *SRO2*, respectively. Plasmid YEpRHO3, which is also an isolate from this library, contains an approximately 10-kb fragment bearing *RHO3*. Plasmid pOPR3 was constructed as follows. A fragment containing the entire *RHO3* coding sequence was amplified by the polymerase chain reaction (32), using the convergent primers that hybridize just upstream of the *RHO3* start codon and just downstream of the stop codon. The resulting fragment was cleaved at the *Eco*RI sites introduced by the primers and inserted at the *Eco*RI site of pKT10 (41), containing *URA3*, the 2μm plasmid origin of replication, and the *TDH3* promoter. This construction placed *RHO3* expression under the control of the *TDH3* promoter. The coding sequence of *RHO3* in pOPR3 was confirmed by sequencing. Plasmids pOPR1 and pOPR2 were constructed in the same way as was pOPR3 except that the entire coding sequences of *RHO1* and *RHO2* (22) were used instead of the *RHO3* coding sequence to construct pOPR1 and pOPR2, respectively. Plasmid pAA7, a gift from T. Fukazawa (Keio University), carries a 274-bp *Bam*HI-*Bgl*II fragment containing the *GAL7* promoter and a 2.5-kb *Bgl*II-*Pvu*II fragment containing the *GAL7* terminator in YEp24 (40). YIpGAL7 was constructed by removing the 2,241-bp *Eco*RI fragment, containing the 2μm plasmid origin of replication, of pAA7. YIpGAL7RHO3 and YIpGAL7RHO4 carry, respectively, an approximately 0.7-kb *Eco*RI fragment containing the entire coding sequence of *RHO3* (derived from pOPR3) and an approximately 0.7-kb *Bam*HI fragment containing the entire coding sequence of *RHO4* (derived from pOPR4 [24]) at the *Bgl*II site in YIpGAL7. Hence, *RHO3* and *RHO4* are expressed under the control of the *GAL7* promoter. YIpGAL7RHO3 and YIpGAL7RHO4 were cleaved at the *Stu*I site in the *URA3* coding sequence and integrated at the *ura3* locus of an appropriate strain. The integrated alleles are designated *pGAL7:RHO3* and *pGAL7:RHO4*, respectively. We transformed diploid strain YPH501 with the *RHO3* deletion plasmid previously described (24) to replace one of the *RHO3* alleles with *rho3::LEU2*, a *rho3* deletion allele. The resultant Leu^+ transformant was transformed to Ura^+ with YIpGAL7RHO4 digested with *Stu*I and was sporulated and dissected to obtain YMR501 and YMR502, segregants carrying *rho3::LEU2 pGAL7:RHO4*. YMR501 was transformed with the *Sma*I fragment carrying *ura3::HIS3*, a *ura3* deletion allele, which was constructed by replacing the internal *Stu*I-*Eco*RV fragment in the 1.1-kb DNA carrying the *URA3* coding sequence with the 1.77-kb *Bam*HI fragment of the *HIS3* gene, to obtain a Ura^- His^+ transformant (YMR505). We transformed YMR501 and YMR502 with the *RHO4* deletion plasmid described previously (24) to replace the *RHO4* allele with *rho4::HIS3*, a *rho4* deletion allele, obtaining YMR509 and YMR510. YMR510 was transformed with the *Sma*I fragment carrying *ura3::TRP1*, a *ura3* deletion allele, which was constructed by replacing the internal *Stu*I-*Eco*RV fragment in the *URA3* coding sequence with the 857-bp *Eco*RI-*Bgl*II fragment of the *TRP1* gene, to obtain Ura^- Trp^+ transformants (YMR512).

Cell lysis. Cell lysis was assayed as described previously (21), with some modifications. In brief, cells were labeled for 12 h at 30°C with [5,6-^{3}H]uracil (1 μCi/ml; 40 Ci/mmol; Dupont) in SCGal-U. Labeled cultures were washed two times with fresh SCGal and were shifted to the desired media with an excess (100 μg/ml) of uracil to quench uptake of labeled uracil. After the shift, the medium was refreshed three times in 2 h to ensure the removal of unincorporated [^{3}H]uracil. Aliquots were fractionated at various times. Cells were removed by centrifugation, and samples from the supernatant fractions were mixed with 5 volumes of Aquasol-2 (Dupont) for liquid scintillation counting. The fraction of labeled material released into the medium was determined

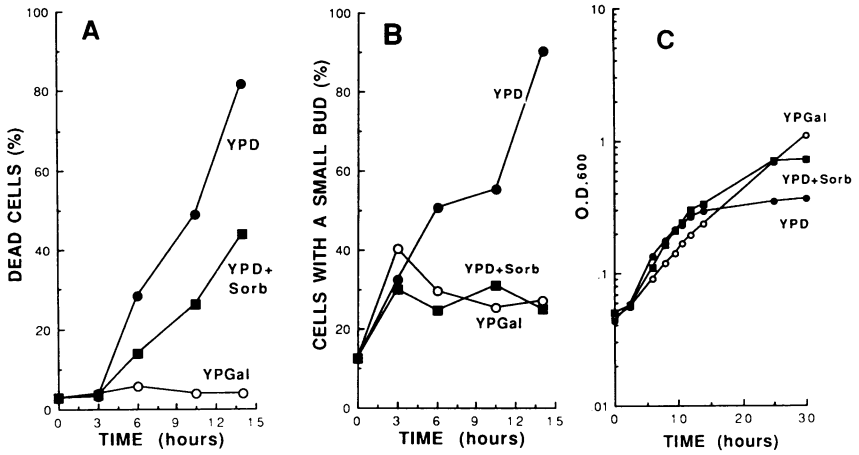

FIG. 1. Effects of Rho3p-Rho4p depletion on cell viability, morphology, and growth. YMR510 cells growing in YPGal were shifted to the media indicated at time zero and incubated at 30°C. (A and B) Cells were harvested at the times indicated and stained with methylene blue. More than 500 cells were observed by microscopy to calculate the number of dead (stained) cells (A) and the number of cells with a bud whose volume is approximately less than one-third of the average volume of wild-type cell buds (B). (C) A portion of the culture was taken at the times indicated, and the optical density at 600 nm ($O.D._{600}$) was measured to estimate the cell mass.

by dividing the disintegrations per minute in the supernatant by the disintegrations per minute in the same volume of the whole culture.

Isolation of multicopy suppressors of the *rho3* defect. YMR505 (*rho3*::*LEU2 pGAL7*:*RHO4*) cultured in YPGal medium was transformed with the *S. cerevisiae* genomic library based on the high-copy-number plasmid YEp24 and plated onto SC-U plates. After 4 days of incubation at 25°C, cells from visible colonies were cultured in YPD individually. Under this condition, YMR505 carrying YEp24 did not form visible colonies on an SC-U plate. Plasmids were recovered from these cultures as described by Sherman et al. (35). To test the ability of plasmids to suppress the *rho3* defect, each plasmid thus isolated was introduced into YMR505 or YMR512, and the transformants were selected on SCGal-U plates and incubated at 25°C until colonies appeared. Several transformants from each transformation were then streaked on an SC-U plate and incubated at 25 or 30°C for 3 to 4 days, and the colony size was measured to estimate suppressing ability. The multicopy suppressors thus recovered were classified by restriction mapping and Southern hybridization.

Morphological observations. Cells were stained with calcofluor (to reveal cell wall chitin), rhodamine-phalloidin (to reveal actin filaments), and 4′,6′-diamidino-2-phenylindole (DAPI) (to reveal DNA) as described previously (30). For DAPI staining, approximately 10^8 cells were harvested, fixed with 70% ethanol, and washed with phosphate-buffered saline (PBS; 140 mM NaCl, 2.7 mM KCl, 3.8 mM Na_2HPO_4). DAPI solution (125 ng/ml in PBS) was applied, and after 1 min at room temperature, cells were washed with PBS. For calcofluor staining, cells were stained with 2 μg of calcofluor per ml in 0.1 M potassium phosphate buffer (pH 7.5). For rhodamine-phalloidin staining, cells were fixed with 5% formaldehyde for 10 min, washed with PBS, stained with 1:50-diluted rhodamine-phalloidin solution (Molecular Probes, Inc.) for 2 h, and washed five times with PBS. These samples were mounted in *n*-propylgallate (10 mg/ml in 90% glycerol) and observed with an epifluorophotomicroscope (Olympus BH-2). Methylene blue staining of yeast cells was performed as described previously (31). Methylene blue solution (0.001% methylene blue, 2% sodium citrate) was mixed with an equal volume of cell culture, and cells were observed immediately with Nomarski optics.

RESULTS

Depletion of both the *RHO3* and *RHO4* proteins results in accumulation of cells with a small bud. As indicated previously (24), *RHO3* is necessary and *RHO4* is dispensable for cell growth; however, the functions of the two genes overlap to some extent. The simultaneous disruption of both *RHO3* and *RHO4* causes a growth defect at 30°C which is suppressed by the overexpression of *RHO4*. To investigate the functions of *RHO3* and *RHO4* during vegetative growth, a strain deleted of both *RHO3* and *RHO4* and carrying a conditionally expressed allele of *RHO4* was constructed. For this purpose, we first constructed *pGAL7*:*RHO4*, a chimeric gene comprising the promoter of the *GAL7* gene fused to the *RHO4* coding sequence, and then introduced it into *rho3*::*LEU2 rho4*::*HIS3* cells. We also constructed the *pGAL7*:*RHO3* allele, the same construct as *pGAL7*:*RHO4* except that the coding sequence of *RHO3* was used instead of that of *RHO4*. However, wild-type cells carrying the *pGAL7*:*RHO3* allele grew slightly more slowly than did wild-type cells without this allele or with the *pGAL7*:*RHO4* allele in galactose medium (data not shown), indicating that expression of *RHO3* with the *GAL7* promoter weakly inhibited cell growth. Since the overexpression of *RHO4* with the *GAL7* promoter showed no deleterious effect on cell growth, the *pGAL7*:*RHO4* allele was used to suppress the loss of the *RHO3* and *RHO4* functions in this study.

Haploid cells (YMR510) and homozygous diploid cells (YMR522) bearing *rho3*::*LEU2*, *rho4*::*HIS3*, and *pGAL7*:*RHO4* grew on YPGal but not on YPD, whereas *rho3*::*LEU2 rho4*::*HIS3* cells without *pGAL7*:*RHO4* did not grow on either medium at 30°C. The viability of YMR510 began to drop about 6 h after the shift to YPD, and the fraction of dead cells increased to about 80% by 14 h after the shift (Fig. 1A), judging from the methylene blue staining; viable cells are not stained, since they take up the dye methylene blue and reduce it to colorless leukomethylene blue, whereas nonviable cells are unable to reduce the dye and therefore are stained blue (31). Essentially the same results were

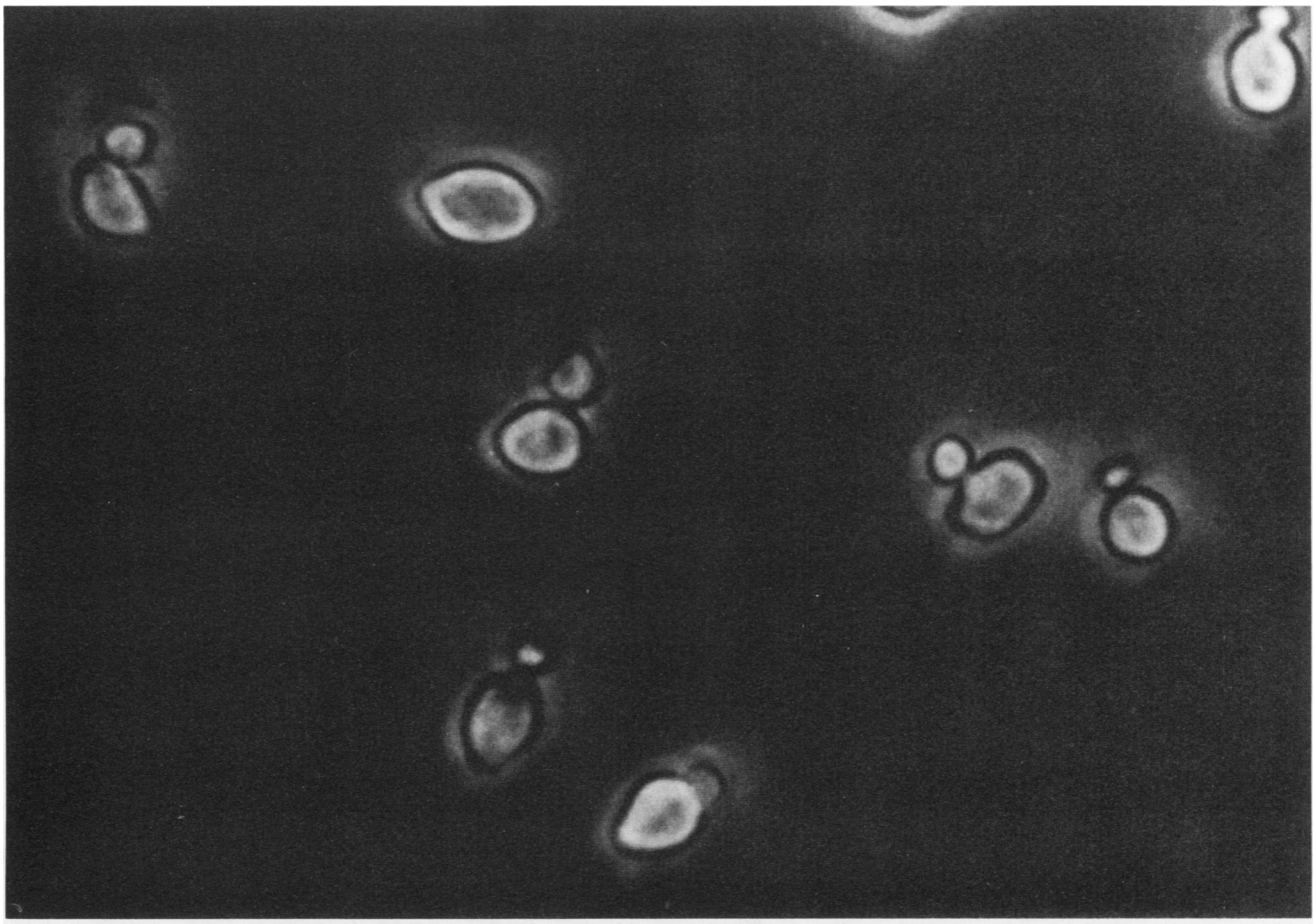

FIG. 2. Morphology of the Rho3p-Rho4p-depleted cells. YMR522 cells growing logarithmically in YPGal at 30°C were shifted to YPD. The photograph was taken at 14 h after the shift. The budded cells were dead, judging from methylene blue staining.

obtained when cell viability was estimated from the efficiency of colony formation on YPGal plates (data not shown). During the cultivation, growth stopped by 14 h after the shift, and up to 90% of the cells had a small bud (Fig. 1B and C). More than 90% of the cells stained with methylene blue possessed a small bud, suggesting that the cells depleted of both the *RHO3* gene product (Rho3p) and the *RHO4* gene product (Rho4p) died at the small-bud stage. Similar results were obtained for diploid strain YMR522. The morphology of the dead cells at 14 h after the shift is shown in Fig. 2.

To examine whether progression of the cell cycle may result in death of the Rho3p-Rho4p-depleted cells, we conducted an experiment using α-factor. YMR512 cells cultured in YPGal were shifted to YPD containing 10 μg of α-factor per ml. During incubation, initiation of bud formation was not observed and projections were formed. The population of the dead cells, judging from methylene blue staining, increased from 8% at 0 h to 25% at 8 h after the shift, while the population of dead cells did not increase in the culture of YMR512 cells shifted to YPGal containing 10 μg of α-factor per ml, suggesting that projection formation kills the Rho3p-Rho4p-depleted cells. In contrast, YMR512 cells arrested in the unbudded state by nitrogen starvation did not die promptly after the shift to glucose-containing medium. YMR512 cells were cultured in SGal lacking a nitrogen source for 3 days for arrest in the unbudded state, and the medium was changed to SD lacking a nitrogen source. The population of dead cells, judging from methylene blue staining, did not increase significantly; the population was 15% at 0 h and 18% at 24 h after the shift. These results suggest that progression of surface growth rather than progression of the cell cycle causes the death of the Rho3p-Rho4p-depleted cells. However, we could not exclude the possibility that depletion of Rho4p did not proceed under conditions of nitrogen starvation. Therefore, the final conclusion on this point awaits studies using a temperature-sensitive *rho3* mutant, which we are trying to isolate.

Rho3p-Rho4p-depleted cells exhibit a cell lysis phenotype. It is possible that the death of cells with a small bud is due to insufficient surface growth of the bud, eventually leading to cell lysis. To test this possibility, we examined whether osmotic stabilizing agents protect Rho3p-Rho4p-depleted cells from death. About 55% of *rho3 rho4 pGAL7:RHO4* cells (YMR510) grown in medium contained 1 M sorbitol were still viable at 14 h after a shift to glucose-containing medium at 30°C, and the mass of cells was increasing, whereas less than 20% of the YMR510 cells were viable without the osmotic stabilizing agent (Fig. 1A and C). In the presence of osmotic stabilizing agents, the population of cells with a small bud did not increase significantly, and the cells stained with methylene blue were not restricted those with a small bud, suggesting that the cells did not always die

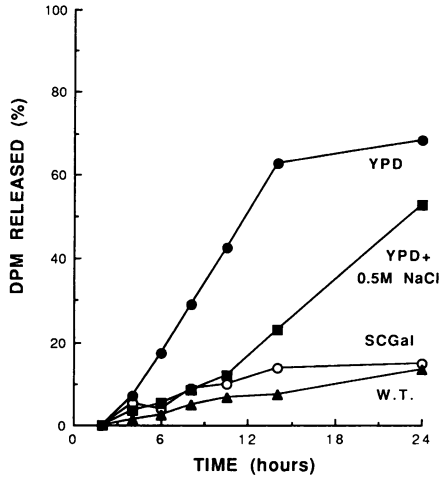

FIG. 3. Lysis of Rho3p-Rho4p-depleted cells. Strain YMR510 (circles and squares) and wild-type (W.T.) strain YPH499 carrying YEp24 (triangles) were labeled with [^{3}H]uracil at 30°C. At time zero, cells were washed, YMR510 cells were shifted to the media indicated, and YPH499 cells were shifted to YPD. Cells were incubated at 30°C. The media were refreshed three times during first 2 h to reduce the background level. Aliquots were taken at the times indicated, and the amount of radioactive material released into the medium was measured.

at the small-bud stage (Fig. 1B). This finding indicates that the osmotic stabilizing agent partially suppresses the lethality of cells with a small bud. Essentially the same results were obtained with use of other osmotic stabilizing agents (0.5 M NaCl, 0.5 M KCl, and 10% polyethylene glycol).

Partial suppression of the lethality of the cells with a small bud by osmotic stabilizing agents suggests that the Rho3p-Rho4p depletion results in lysis of cells with a small bud. To clarify this point, we examined the release of radioactive material from cells labeled with [^{3}H]uracil. *rho3 rho4 pGAL7:RHO4* cells (YMR510) started to release their radioactive material into the medium by 6 h after a shift to YPD and released 60% of total label by 14 h after the shift, reaching a plateau (Fig. 3). The time course of the release of intracellular material is coincident with the increase of the population of dead cells with a small bud (Fig. 1B), strongly suggesting that the Rho3p-Rho4p depletion results in lysis of cells with a small bud. In YPD containing 0.5 M NaCl as an osmotic stabilizing agent, the cells released only about 20% of their radioactive material into the medium after 14 h; however, the leakage continued, and about 50% of the material was released into the medium after 24 h, indicating that osmotic stabilizing agents partially blocked cell lysis.

Rho3p-Rho4p-depleted cells lose cell polarity. Although YMR522 cells depleted both Rho3p and Rho4p promptly died in medium without an osmotic stabilizing agent, considerable fractions of the cells remained alive in the presence of an osmotic stabilizing agent at 14 h after a shift to glucose-containing medium. This phenomenon enabled us to observe the events taking place after removal of Rho3p and Rho4p from living cells. YMR522 cells cultured in YPD+Sorb lost their oval shape and were enlarged and rounded (Fig. 4C), in contrast to the normal shape of YMR522 cells grown in YPGal+Sorb (Fig. 4A). The cell wall chitin was localized predominantly to the bud neck in YMR522 cells grown in YPGal+Sorb (Fig. 4B). In contrast, those grown in YPD+Sorb deposited chitin throughout the cell surface (Fig. 4D). The difference of distribution of deposited chitin between glucose-grown cells and galactose-grown cells is more apparent in Fig. 4F; in this case, YMR522 cells cultured in either condition were mixed and stained with calcofluor. The rounded cells from the YPD+Sorb culture and the oval-shaped cells from the YPGal+Sorb culture were readily distinguished (Fig. 4E), and the delocalization of chitin deposition was specific for the rounded cells (Fig. 4F).

Asymmetric distribution of actin, the actin patches concentrated in the buds and actin cables running through the mother cells into the buds, was observed in wild-type cells (Fig. 5A) and in YMR522 cultured in YPGal containing 0.5 M KCl as an osmotic stabilizing agent (Fig. 5B). In contrast, YMR522 cultured in YPD with the osmotic stabilizing agent displayed a random distribution of actin patches (Fig. 5C and D). The alteration of actin distribution is not due to cell lysis, since we did not observe any structure stained with rhodamine-phalloidin in cells killed by lysis. These results indicate that the Rho3p-Rho4p-depleted cells incubated in the presence of an osmotic stabilizing agent lost cell polarity. DAPI staining of these cells revealed that about 20% of the cells became multinucleated (Fig. 5E and F), indicating that the nuclear cycle was continuing. These phenotypes shown by the Rho3p-Rho4p-depleted cells are quite similar to those of mutants in bud emergence, such as *cdc24* and *cdc42* cells, except that the Rho3p-Rho4p-depleted cells cultured with an osmotic stabilizing agent often have a bud, whereas the bud emergence mutants are unbudded at restrictive temperatures.

Isolation of multicopy suppressors of the *rho3* defect. To explore the *RHO3* and *RHO4* functions further, we screened a high-copy-number yeast genomic library for genes whose overexpression could suppress the *rho3* defect. We transformed strain YMR505 (*rho3::LEU2 pGAL7:RHO4 ura3*) to Ura$^+$ at 25°C on SC-U plates with a yeast genomic DNA library constructed in the high-copy-number plasmid YEp24. We obtained 31 transformants that could grow on glucose-containing plates. From each of these 31 transformants, plasmids were recovered into *E. coli* for further analysis. Five of these 31 plasmids failed to suppress the growth defect of YMR505 on SC-U plates when they were introduced into YMR505 again, indicating that the suppression event in them at the time of screening was not due to the plasmids. By restriction analysis and Southern hybridization, the other plasmids, carrying the suppressing activity, were classified into 10 groups, each containing a different suppressor gene. One of them contained *RHO3* itself. The other genes were designated *SRO1~9* (suppressor of *rho3*). The cumulative number of the isolates and the suppressing activity of each isolate are summarized in Table 2. Extensive screening will identify *SRO* genes other than *SRO1~9*, since *RHO4*, a multicopy suppressor of the *rho3* defect, was not found among *SRO1~9*. These *SRO* genes are divided into two classes according to the ability to complement the *rho3* or *rho3 rho4* deletion. Genes in class I (*SRO1~5*), when overexpressed, complemented not only the deletion of *RHO3* but also the simultaneous deletion of both *RHO3* and *RHO4*. Overexpression of genes in class II (*SRO6~9*) complemented only the *rho3* defect, and the ability to suppress the *rho3 rho4* defect was very weak if present at all. Characterization of *SRO3~9* will be described elsewhere Suppressing activities of *SRO1* and *SRO2* are shown in Fig. 6. A high dose of *SRO1* or *SRO2* suppressed the growth defect of both YMR505 and YMR512 on a glucose-containing plate.

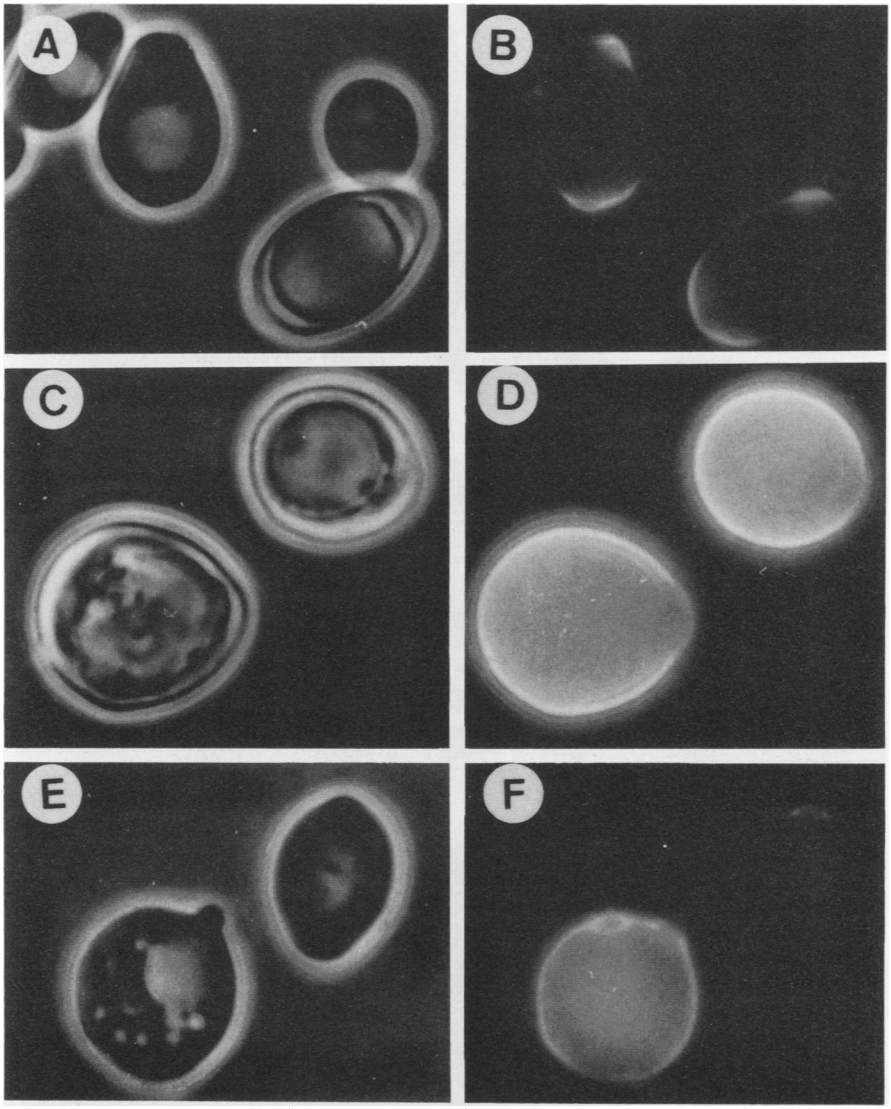

FIG. 4. Delocalization of deposition of chitin in Rho3p-Rho4p-depleted cells. YMR522 cells growing logarithmically in YPGal+Sorb at 30°C were shifted to YPGal+Sorb (A and B) and YPD+Sorb (C and D), and incubation was continued at 30°C for 14 h. Equal volumes of the YPGal+Sorb and YPD+Sorb cultures were mixed (E and F) and processed for microscopic observation. Cells were stained with calcofluor and photographed with a phase-contrast (A, C, and E) or fluorescence (B, D, and F) microscope.

The DNA fragments carrying *SRO1* and *SRO2* were digested with appropriate restriction enzymes and inserted into the multicloning site of pBluescript for sequencing and into YEp24 for determination of the region responsible for the suppressing ability. The restriction maps of *SRO1* and *SRO2* and the regions carrying *rho3* defect-suppressing activity are diagrammed in Fig. 7. The restriction map of *SRO1* was identical with that of *BEM1* (Fig. 7), and the nucleotide sequence in the coding region of *SRO1* was identical with that of *BEM1* (data not shown). The restriction map of *SRO2* was identical with that of *CDC42* diagrammed in Fig. 7. The determined nucleotide sequence near the *Hpa*I site of *SRO2* was identical with that of *CDC42* (data not shown). The coding region of *SRO1* corresponding to that of *BEM1* and the coding region of *SRO2* corresponding to that of *CDC42* were essential for suppression of the *rho3* defect (Fig. 7). Therefore, we concluded that *SRO1* and *SRO2* are identical with *BEM1* and *CDC42*, respectively.

YMR512 (*rho3*::*LEU2 rho4*::*HIS3 pGAL7*:*RHO4*) with a high-copy-number plasmid carrying either *CDC42* or *BEM1* was cultured in glucose medium. More than 80% of the cells of these cultures showed wild-type-like cell shape and cell size, and chitin deposition was localized predominantly around the bud neck (data not shown), indicating that the loss of cell polarity in the *rho3 rho4* cells was suppressed by the high dose of either *BEM1* or *CDC42*.

CDC42 is a member of *rho* family genes. To test whether high doses of any *rho* family genes suppress the *rho3* defect, we constructed plasmids pOPR1 and pOPR2, in which *RHO1* and *RHO2*, respectively, were expressed under the control of the *TDH3* promoter, and these plasmids were individually introduced into YMR505 and YMR512 to assay suppression of the *rho3* defect. Neither pOPR1 nor pOPR2 suppressed the growth defect of YMR505 and YMR512 on a glucose-containing medium (data not shown), indicating that the functions of *RHO1* and *RHO2* could not substitute for

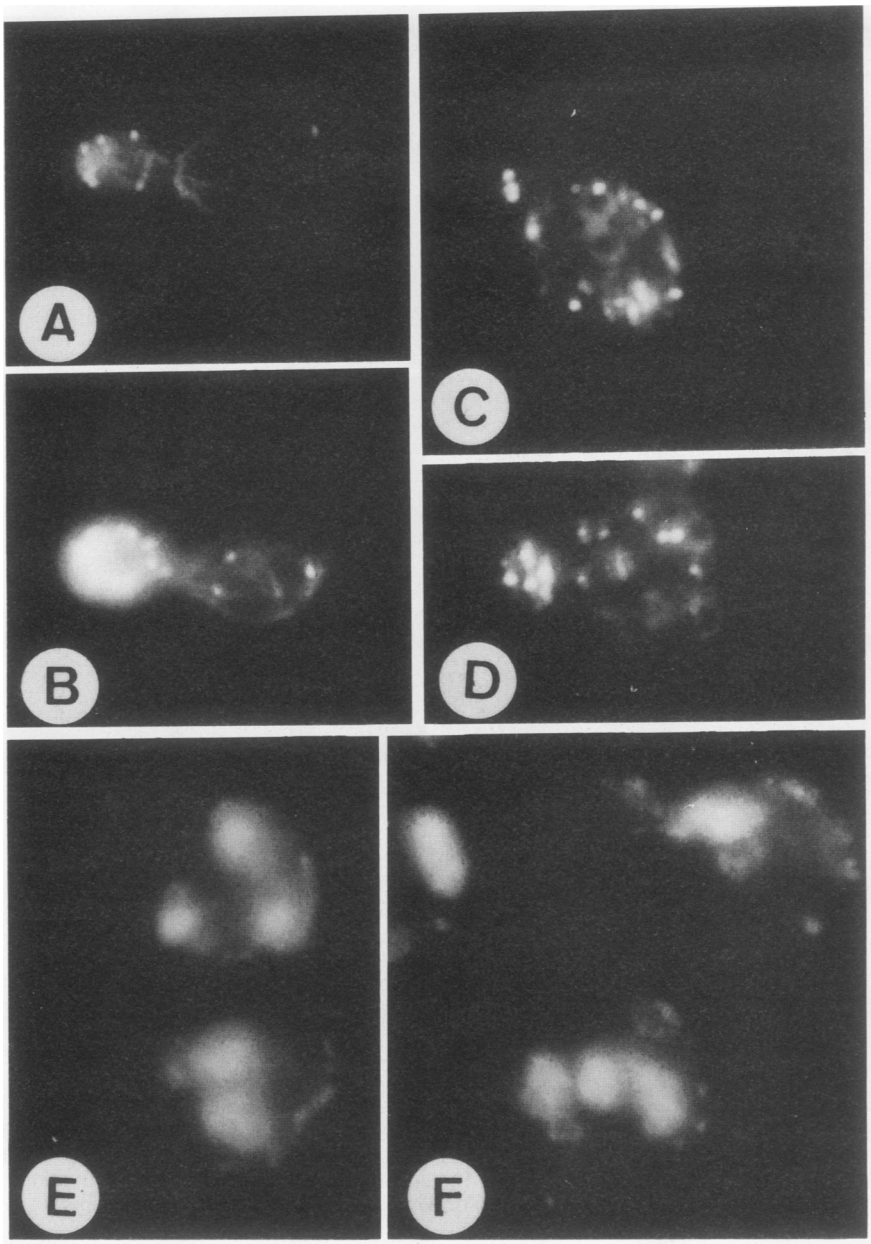

FIG. 5. Rhodamine-phalloidin staining and DAPI staining of Rho3p-Rho4p-depleted cells. Wild-type strain YPH501 (A), strain YMR522 grown in YPGal containing 0.5 M KCl (B), strain YMR522 shifted to YPD containing 0.5 M KCl as an osmotic stabilizing agent and incubated at 30°C for 14 h (C to F) were fixed. (A to D) Cells stained with rhodamine-phalloidin to reveal actin; (E and F) cells stained with DAPI.

the *RHO3* function. This finding suggests that the similarity of primary structure alone is not sufficient for suppressing the *rho3* defect.

Overexpression of *RHO3* had an inhibitory effect on the growth of mutants defective in bud emergence. The fact that the high dose of *CDC42* or *BEM1*, genes involved in bud emergence, suppressed the defect of the *RHO3* and *RHO4* functions gave us some clues about the functions of *RHO3* and *RHO4* in bud emergence. To investigate this matter further, we tested whether overexpression of *RHO3* suppresses the defect in bud emergence. YEpRHO3, a high-copy-number plasmid carrying *RHO3*, was introduced into Y147, a strain carrying a *cdc24-4* mutation (defective in bud emergence at restrictive temperatures). Y147 carrying YEpRHO3 did not grow at 34°C (Fig. 8b, sector A), whereas Y147 with a high-copy-number plasmid carrying *CDC42* did (Fig. 8, sector B). This result indicates that the high dose of *RHO3* did not complement *cdc24-4*. Similarly, the high dose of *RHO3* did not complement the *cdc42-1* temperature-sensitive mutation, since introduction of YEpRHO3 into YMR420, a *cdc42-1* strain, did not affect its restrictive temperature (data not shown).

For higher expression of *RHO3*, pOPR3, a multicopy plasmid carrying the *RHO3* coding sequence under the control of the *TDH3* promoter, was constructed and was introduced into Y147. Overexpression of *RHO3* with the *TDH3* promoter inhibited the growth of Y147 at 30°C (Fig. 8a, sector C), whereas Y147 carrying control plasmid pKT10

TABLE 2. Isolation of multicopy suppressors (*SRO* genes)

Gene	No. of independent isolates	Suppressing activity[a]	
		rho3	*rho3 rho4*
SRO1	3	++	++
SRO2	2	+	+
SRO3	1	+	++
SRO4	1	+	+
SRO5	1	+	+
SRO6	5	+++	+/−
SRO7	1	+++	−
SRO8	1	++	−
SRO9	1	++	−
RHO3	3	++++	++++

[a] Ranged from allowing no detectable growth (−) to allowing essentially normal growth (++++).

grew normally (Fig. 8a, sector D). Furthermore, the existence of pOPR3 may be incompatible with the *cdc42-1* mutation, since we could not obtain any transformant of YMR420 with pOPR3 even at 25°C. The overexpression of *RHO3* by the *GAL7* promoter also seemed to inhibit the growth of YMR420, since the restrictive temperature of YMR420 carrying *pGAL7:RHO3* was reduced to 32°C in YPGal, whereas that of YMR420 without this allele was 35°C in YPGal (data not shown). These results are in contrast to the fact that wild-type cells carrying pOPR3 grew slightly more slowly than did those carrying YEp24 but did not show any temperature-sensitive growth. Overexpression of *RHO4* under control of the *PYK1* promoter (27) did not affect the restrictive temperature of YMR420 (data not shown), suggesting that overexpression of *RHO4* neither complements *cdc42-1* nor inhibits the growth of *cdc42-1* mutant cells.

DISCUSSION

In this study, we found that depletion of the *RHO3* and *RHO4* functions results in lysis of cells with a small bud and that this cell lysis defect is partially suppressed by an osmotic stabilizing agent, such as 1 M sorbitol, 0.5 M NaCl, 0.5 M KCl, or 10% polyethylene glycol (Fig. 1 and 3). These results suggest that the *RHO3* and *RHO4* functions are required to confer osmotic resistance on a newly formed cell by stimulating surface growth at the bud site. Since yeast cells show secretion polarized toward the budding site and since deposition of new cell wall material is essential for bud formation, it is likely that the cell lysis mentioned above is the result of insufficient transport of material for surface growth due to the loss of cell polarity in the Rho3p-Rho4p-depleted cells. This hypothesis is strongly supported by the fact that the Rho3p-Rho4p-depleted cells lost cell polarity (Fig. 4 and 5). Loss of cell polarity is reported in cells with bud emergence mutations such as *cdc24* and *cdc42* (1, 38). However, the morphology of the Rho3p-Rho4p-depleted cells is distinct from that of the bud emergence mutants, in that the Rho3p-Rho4p-depleted cells arrest as cells with a small bud in the absence of osmotic stabilizing agents,

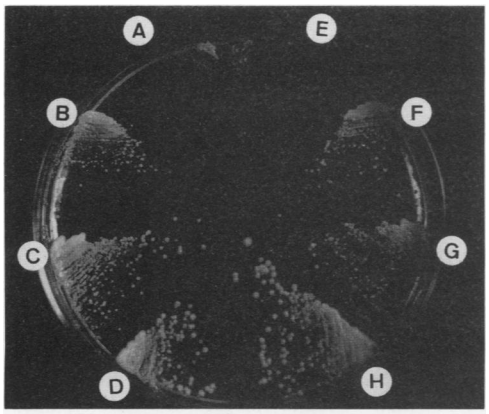

FIG. 6. Suppression of the *rho3* defect by high doses of *SRO1* and *SRO2*. *rho3::LEU2 pGAL7:RHO4* strain YMR505 (A to D) and *rho3::LEU2 rho4::HIS3 pGAL7:RHO4* strain YMR512 (E to H) were transformed with control plasmid YEp24 (A and E), pSRO2 (B and F), pSRO1 (C and G), or YEpRHO3 (D and H) and plated on SCGal-U. The transformants were streaked on a YPD plate and incubated at 30°C for 3 days.

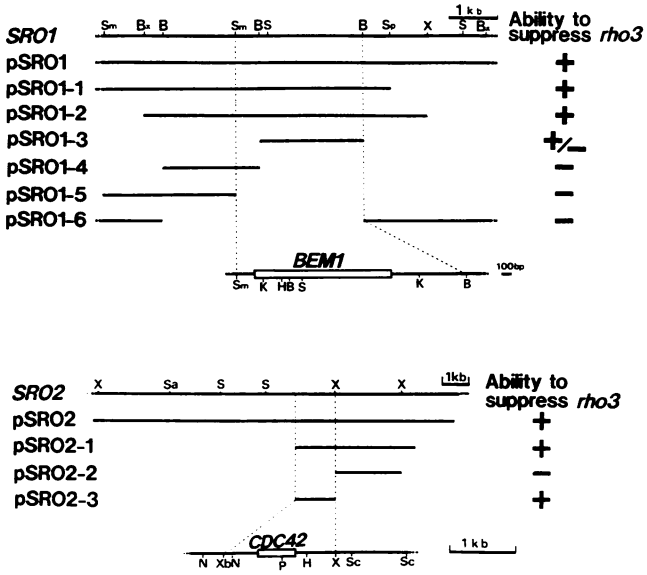

FIG. 7. Restriction maps of *SRO1* and *SRO2* and of the clones and subclones derived from them. The restriction maps confirmed to be identical with those of *BEM1* (11) and *CDC42* (20) are enlarged and shown below the maps. The coding regions are represented by open boxes. pSRO1, pSRO2, and pSRO2-1 were the primary isolates from the YEp24 library. pSRO1-1 was constructed by deleting the 2.3-kb *SplI* fragment from pSRO1. For the construction of pSRO1-2, pSRO1 was digested with *XhoI* and *PvuII*, filled in, and ligated and then digested with *BstXI* and *NheI*, filled in, and ligated. pSRO1-3 was constructed by inserting the 2.2-kb *BamHI* fragment of pSRO1 into the *BamHI* site of YEp24. pSRO1-4 was constructed by inserting the 2.0-kb *BamHI* fragment of pSRO1 into the *BamHI* site of YEp24. pSRO1-5 was constructed by inserting the 2.9-kb *SmaI* fragment of pSRO1 into the *SmaI* site of YEp24. pSRO1-6 was constructed by deleting the 4.2-kb *BamHI* fragment from pSRO1. For the construction of pSRO2-3, pSRO2-1 was digested with *XhoI* and *SmaI*, filled in, and ligated. pSRO2-2 was constructed by inserting the 2.5-kb *XhoI* fragment from pSRO2-1 into the *SalI* site of YEp24. The suppressing activity of each plasmid was determined by the method described in the text. +, transformants formed visible colonies after incubation for 3 days at 25°C; −, no visible colonies appeared after incubation for 3 days at 25°C; +/−, transformants exhibited weak suppression (the transformant colonies were slightly larger than those with control plasmid YEp24 after incubation for 5 days at 25°C). B, *BamHI*; Bx, *BstXI*; H, *HpaI*; K, *KpnI*; N, *NdeI*; P, *PvuI*; S, *SalI*; Sa, *SacI*; Sc, *ScaI*; Sp, *SplI*; X, *XhoI*; Xb, *XbaI*.

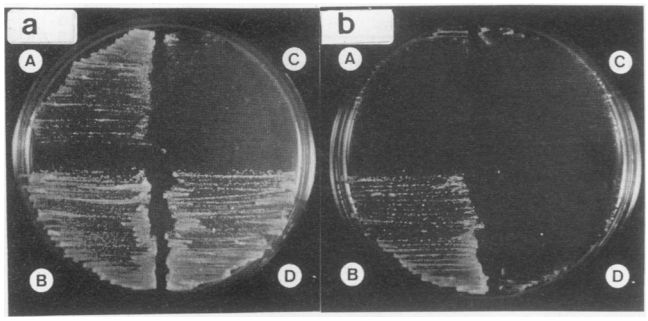

FIG. 8. Effect of overexpression of *RHO3* in a *cdc24-4* strain. *cdc24-4* strain Y147 was transformed with YEpRHO3, a multicopy plasmid carrying RHO3 (A), pSRO2, a multicopy plasmid carrying *CDC42* (B), pOPR3, a multicopy plasmid carrying the *RHO3* coding sequence under the control of the *TDH3* promoter (C), or pKT10, a control plasmid (D). Transformants were streaked on an SC-U plate and incubated at 30°C (a) or 34°C (b) for 2 days.

whereas the bud emergence mutants become unbudded, enlarged, and rounded cells at the restrictive temperature. These facts indicate that Rho3p-Rho4p-depleted cells initiate bud emergence and then lose cell polarity. Once cells initiate budding, the bud site becomes sensitive to osmotic pressure unless polarized transport of materials proceeds normally. The fact that the Rho3p-Rho4p-depleted cells lost viability after producing a bud strongly suggest that there is an essential stage for bud growth after initiation of bud emergence. We call this step maintenance of cell polarity.

Presumably, budding requires formation of a complex of the gene products of bud site assembly genes, such as *CDC42*, *CDC24*, and *BEM*, at the bud site and recruitment of these gene products at the bud site so that surface growth is restricted to the bud (13). Since initiation of bud formation may be the result of the assembly of this complex (bud site complex), the maintenance of cell polarity may correspond to the maintenance and development of the bud site complex, which is probably needed for bud growth. Judging from the phenotype of the Rho3p-Rho4p-depleted cells (Fig. 4 and 5), Rho3p and Rho4p play a pivotal role in maintenance and development of the bud site complex. Therefore, it is possible that the gene products of the multicopy suppressors of the *rho3* defect are the components of the bud site complex or positive regulators of the assembly process, since elevated concentrations of these factors may restore assembly of the bud site complex without the *RHO3* function. This hypothesis is strongly supported by the fact that *SRO1* and *SRO2* are identical with *CDC42* and *BEM1*, respectively, which are bud site assembly genes (13).

Since the *BEM1* gene product possesses two SH3 domains, this protein might link actin of the cytoskeleton to the bud site complex (11). Functional interaction of *BEM1* with other genes that may be required for assembly of the bud site complex, such as *BUD5* (9), *MSB1* (5), and *SPA2* (12), along with the fact that the *BEM1* gene product possesses two SH3 domains, suggests that the *BEM1* gene product performs a key function in assembly of the bud site complex. The fact that a high dose of *BEM1* suppresses the *rho3 rho4* defect suggests that the *BEM1* gene product is a candidate for the factor whose assembly in the bud site complex is regulated by the *RHO3* and *RHO4* functions.

It is conceivable that the *CDC42* gene product is a positive regulator of the assembly of the bud site complex (1, 13, 43). Therefore, a high dose of *CDC42* may contribute to maintaining the complex in the absence of Rho3p and Rho4p. Functional interaction between *CDC42* and *MSB1* (4), along with the genetic interaction between *BEM1* and *MSB1* (5), suggests the possibility that *CDC42* suppresses the *rho3 rho4* defect through the functions of *MSB1* and/or *BEM1*.

These arguments place the functions of *CDC42* and *BEM1* downstream of, in the same position as, or overlapping those of *RHO3* and *RHO4*. However, morphological observation of the Rho3p-Rho4p-depleted cells indicated that the *RHO3* and *RHO4* functions are needed after bud initiation. To reconcile these facts, we assume that the gene products of *CDC42* and *BEM1* are also involved in maintenance of cell polarity, cooperating with Rho3p and Rho4p.

To form a daughter cell, bud enlargement, as well as the previous two successive processes, selection of a bud site and initiation of bud formation, is necessary. Selection of a bud site and initiation of bud emergence are controlled by the *ras* superfamily genes *RSR1* (4, 10) and *CDC42* (1, 20), respectively. In this study, we found that the *ras* superfamily genes *RHO3* and *RHO4* are also necessary for bud enlargement. It is interesting that the successive process of bud growth is regulated by interaction among the specific *ras* superfamily genes. Overexpression of *CDC42* suppresses the *rho3* defect, whereas overexpression of *RHO3* has an inhibitory effect on the *CDC24-CDC42* pathway. Overexpression of *RSR1* suppresses the defect of *cdc24*, while overexpression of *CDC42* perturbs selection of the bud site (4, 20). These data indicate that there is a network of functional interactions among these *ras* superfamily gene products, probably through sharing of an interacting molecule(s), such as an exchange factor and a GTPase-activating protein (GAP), among these *ras* superfamily gene products and/or the interaction among these regulatory molecules. Fine control of these *ras* superfamily gene products through this network ensures that the cell will carry out the budding process unidirectionally. In mammalian systems, a wide spectrum of substrate specificity of the regulatory molecules and direct interaction between GAP and a GAP-related protein have been reported (18, 25, 34), suggesting functional interactions among *ras* superfamily gene products. Studies of regulation of the assembly of the bud site complex will shed some light on this matter. Characterization of the *SRO* gene products will reveal the regulators required for assembly of the bud site complex and will also enable us to dissect the components of this complex.

ACKNOWLEDGMENTS

We thank R. Matsui for technical assistance. We also thank R. B. Wickner for critical reading of the manuscript.

Part of this work was supported by a grant for scientific work from Monbusho.

REFERENCES

1. **Adams, A. E. M., D. I. Johnson, R. M. Longnecker, B. F. Sloat, and J. R. Pringle.** 1990. *CDC42* and *CDC43*, two additional genes involved in budding and the establishment of cell polarity in the yeast *Saccharomyces cerevisiae*. J. Cell Biol. **111**:131–142.
2. **Adams, A. E. M., and J. R. Pringle.** 1984. Relationship of actin and tubulin distribution to bud growth in wild-type and morphogenetic-mutant *Saccharomyces cerevisiae*. J. Cell Biol. **98**:934–945.
3. **Barbacid, M.** 1987. *ras* genes. Annu. Rev. Biochem. **55**:779–827.
4. **Bender, A., and J. R. Pringle.** 1989. Multicopy suppression of the *cdc24* budding defect in yeast by *CDC42* and three newly identified genes including the *ras*-related *RSR1* gene. Proc.

Natl. Acad. Sci. USA **86**:9976–9980.
5. **Bender, A., and J. R. Pringle.** 1991. Use of screen for synthetic lethal and multicopy suppressee mutants to identify two new genes involved in morphogenesis in *Saccharomyces cerevisiae*. Mol. Cell. Biol. **11**:1295–1305.
6. **Botstein, D., S. C. Falco, S. E. Stewart, M. Brennan, S. Scherer, D. T. Stinchcomb, K. Struhl, and R. W. Davis.** 1979. Sterile host yeasts (SHY): a eukaryotic system of biological containment for recombinant DNA experiments. Gene **8**:17–24.
7. **Cabib, E., R. Roberts, and B. Bowers.** 1982. Synthesis of the yeast cell wall and its regulation. Annu. Rev. Biochem. **51**:763–793.
8. **Carlson, M., and D. Botstein.** 1982. Two differentially regulated mRNAs with different 5′ ends encode secreted and intracellular forms of yeast invertase. Cell **28**:145–154.
9. **Chant, J., K. Corrado, J. R. Pringle, and I. Herskowitz.** 1991. The yeast *BUD5* gene, which encodes a putative GDP-GTP exchange factor, is necessary for bud-site selection and interact with bud-formation gene *BEM1*. Cell **65**:1213–1224.
10. **Chant, J., and I. Herskowitz.** 1991. Genetic control of bud site selection in yeast by a set of gene products that constitute a morphogenetic pathway. Cell **65**:1203–1212.
11. **Chenevert, J., K. Corrado, A. Bender, J. Pringle, and I. Herskowitz.** 1992. A yeast gene (*BEM1*) necessary for cell polarization whose product contains two SH3 domains. Nature (London) **356**:77–79.
12. **Costigan, C., S. Gehrung, and M. Snyder.** 1992. A synthetic lethal screen identifies SLK1, a novel protein kinase homolog implicated in yeast cell morphogenesis and cell growth. Mol. Cell. Biol. **12**:1162–1178.
13. **Drubin, D. G.** 1991. Development of cell polarity in budding yeast. Cell **65**:1093–1096.
14. **Field, C., and R. Schekman.** 1980. Localized secretion of acid phosphatase reflects the pattern of cell surface growth in *Saccharomyces cerevisiae*. J. Cell Biol. **86**:123–128.
15. **Hart, M. J., A. Eva, T. Evans, S. A. Aaronson, and R. A. Cerione.** 1991. Catalysis of guanine nucleotide exchange on the CDC42Hs protein by the *dbl* oncogene product. Nature (London) **354**:311–314.
16. **Hartwell, L. H., J. Culotti, J. R. Pringle, and B. J. Reid.** 1974. Genetic control of the cell division cycle in yeast. Science **183**:46–51.
17. **Henikoff, S.** 1984. Unidirectional digestion with exonuclease III creates targeted breakpoints for DNA sequencing. Gene **28**:351–359.
18. **Hiraoka, K., K. Kaibuchi, S. Ando, T. Musha, K. Takaishi, T. Mizuno, M. Asada, L. Menard, E. Tomhave, J. Didsbury, R. Snyderman, and Y. Takai.** 1992. Both stimulatory and inhibitory GDP/GTP exchange proteins, *smg* GDS and *rho* GDI, are active on multiple small GTP-binding proteins. Biochem. Biophys. Res. Commun. **182**:921–930.
19. **Ito, H., Y. Fukuda, K. Murata, and A. Kimira.** 1983. Transformation of intact yeast cells treated with alkali cations. J. Bacteriol. **153**:163–168.
20. **Johnson, D. I., and J. R. Pringle.** 1990. Molecular characterization of *CDC42*, a *Saccharomyces cerevisiae* gene involved in the development of cell polarity. J. Cell Biol. **111**:143–152.
21. **Lee, K. S., and D. E. Levin.** 1992. Dominant mutations in a gene encoding a putative protein kinase (*BCK1*) bypass the requirement for a *Saccharomyces cerevisiae* protein kinase C homolog. Mol. Cell. Biol. **12**:172–182.
22. **Madaule, P., R. Axel, and A. M. Myers.** 1987. Characterization of two members of the *rho* gene family from the yeast *Saccharomyces cerevisiae*. Proc. Natl. Acad. Sci. USA **84**:779–783.
23. **Maniatis, T., E. F. Fritsch, and J. Sambrook.** 1982. Molecular cloning: a laboratory manual. Cold Spring Harbor Laboratory, Cold Spring Harbor, N.Y.
24. **Matsui, Y., and A. Toh-e.** Isolation and characterization of two novel *ras* superfamily genes in *Saccharomyces cerevisiae*. Gene **114**:43–49.
25. **Mizuno, T., K. Kaibuchi, T. Yamamoto, M. Kawamura, T. Sakoda, H. Fujioka, Y. Matsuura, and Y. Takai.** 1991. A stimulatory GDP/GTP exchange protein for smg p21 is active on the post-translationally processed form of c-Ki-ras p21 and rhoA p21. Proc. Natl. Acad. Sci. USA **88**:6442–6446.
26. **Munemitsu, S., M. A. Innis, R. Clark, F. McCormick, A. Ullrich, and P. Polakis.** 1990. The molecular cloning and expression of G25K, the human homolog of the yeast cell cycle gene *CDC42*. Mol. Cell. Biol. **10**:5977–5982.
27. **Nishizawa, M., R. Araki, and Y. Teranishi.** 1989. Identification of upstream activating sequences and an upstream repressible sequence of the pyruvate kinase gene of the yeast *Saccharomyces cerevisiae*. Mol. Cell. Biol. **9**:442–451.
28. **Pringle, J. R., and L. H. Hartwell.** 1981. The *Saccharomyces cerevisiae* cell cycle, p. 97–142. *In* J. N. Strathern, J. R. Broach, and E. W. Jones (ed.), The molecular biology of the yeast *Saccharomyces*: life cycle and inheritance. Cold Spring Harbor Laboratory, Cold Spring Harbor, N.Y.
29. **Pringle, J. R., S. H. Lillie, A. E. M. Adams, C. W. Jacobs, B. K. Haarer, K. G. Coleman, J. S. Robinson, L. Bloom, and R. A. Preston.** 1986. Cellular morphogenesis in the yeast cell cycle, p. 47–80. *In* J. Hicks (ed.), Yeast cell biology. Alan R. Liss Inc., New York.
30. **Pringle, J. R., R. A. Preston, A. E. M. Adams, T. Stearns, D. Drubin, B. K. Haarer, and E. W. Jones.** 1989. Fluorescence microscopy methods for yeast. Methods Cell Biol. **31**:357–435.
31. **Rose, A. H.** 1975. Growth and handling of yeasts. Methods Cell Biol. **12**:1–15.
32. **Saiki, R. K., D. H. Gelfand, S. Stoffel, S. L. Scharf, R. Higuchi, G. T. Horn, K. B. Mullis, and H. A. Erlich.** 1988. Primer-directed enzymatic amplification of DNA with a thermostable DNA polymerase. Science **239**:487–491.
33. **Sanger, F., S. Nicklen, and A. R. Coulson.** 1977. DNA sequencing with chain-terminating inhibitors. Proc. Natl. Acad. Sci. USA **74**:5463–5467.
34. **Settleman, J., V. Narasimhan, L. C. Foster, and R. A. Weinberg.** 1992. Molecular cloning of cDNAs encoding the GAP-associated protein p190: implications for a signaling pathway from ras to the nucleus. Cell **69**:539–550.
35. **Sherman, F., G. R. Fink, and J. B. Hicks.** 1986. Methods in yeast genetics. Cold Spring Harbor Laboratory, Cold Spring Harbor, N.Y.
36. **Shinjo, K., J. G. Koland, M. J. Hart, V. Narasimhan, D. I. Johnson, T. Evans, and R. Cerione.** 1990. Molecular cloning of the gene for the human placental GTP-binding protein Gp (G25K): identification of this GTP-binding protein as the human homolog of the yeast cell-division-cycle protein CDC42. Proc. Natl. Acad. Sci. USA **87**:9853–9857.
37. **Sikorski, R. S., and P. Hieter.** 1989. A system of shuttle vector and yeast host strains designed for efficient manipulation of DNA in *Saccharomyces cerevisiae*. Genetics **122**:19–27.
38. **Sloat, B. F., A. E. M. Adams, and J. R. Pringle.** 1981. Role of the *CDC24* gene product in cellular morphogenesis during the *Saccharomyces cerevisiae* cell cycle. J. Cell Biol. **89**:395–405.
39. **Sloat, B. F., and J. R. Pringle.** 1978. A mutant of yeast defective in cellular morphogenesis. Science **200**:1171–1173.
40. **Tajima, M., Y. Nogi, and T. Fukazawa.** 1986. Duplicate upstream activating sequences in the promoter region of the *Saccharomyces cerevisiae GAL7* gene. Mol. Cell. Biol. **6**:246–256.
41. **Tanaka, K., K. Matsumoto, and A. Toh-e.** 1988. Dual regulation of the expression of the polyubiquitin gene by cyclic AMP and heat shock in yeast. EMBO J. **7**:495–502.
42. **Tkacz, J. S., and J. O. Lampen.** 1973. Surface distribution of invertase on growing *Saccharomyces* cells. J. Bacteriol. **113**: 1073–1075.
43. **Zimam, M., J. M. O'Brien, L. A. Ouellette, W. R. Church, and D. I. Johnson.** 1991. Mutational analysis of *CDC42Sc*, a *Saccharomyces cerevisiae* gene that encodes a putative GTP-binding protein involved in the control of cell polarity. Mol. Cell. Biol. **11**:3537–3544.